JOURNAL OF MATERIALS SCIENCE 10 (1975) 136-158

Review
Microstructural control in lead alloys for storage battery application

JEFF PERKINS*, G. R. EDWARDS
Materials Science Group, Department of Mechanical Engineering, Naval Postgraduate School, Monterey, California, USA

The role of alloying and thermomechanical processing in direct microstructural control in lead-base storage battery alloys is reviewed. Strength, corrosion, and electrochemical correlations are discussed for conventional and emerging lead alloy systems.

1. Introduction

Lead-antimony alloys have been widely used as the grid metal for lead-acid batteries for many years [1]. Unfortunately, antimony has deleterious electrochemical side effects [2, 3] in addition to its useful strengthening role. In service, antimony migrates to the negative plate, lowering the hydrogen overvoltage and leading to excessive gassing and loss of electrolyte upon charge. (In addition to this problem, the cost of antimony has increased greatly in the last few years.) With the advent of a large potential market for so-called "maintenance-free" batteries [4-6] (i.e. sealed; no addition of water required over life of battery; high end-of-charge voltage; low self-discharge), the use of lead-calcium alloys has been investigated [7-14]. These alloys do not have the electrochemical problems of antimony bearing alloys, but have other drawbacks. They are somewhat weaker than antimonal alloys, and are difficult to cast, requiring high mould temperatures which slow production rates. The higher temperatures also tend to promote oxidation of the melt, so that nominal compositions may deviate due to dross losses of alloying elements. Calcium alloys are also subject to a form of intergranular corrosion which causes shortened service life (and requires grain size control to be paid close attention). In addition, calcium alloys require a very high voltage in order to recharge after a deep discharge [15]; in fact, the voltage required may be higher than that available with normal charging equipment, so that the battery must be discarded. This phenomena is attributable to passivation of the grid surface by formation of a nonconductive corrosion product layer during discharge [10, 11]. For this reason, tin is usually added to the alloy composition to enable easier recovery from deep discharge, (as well as additional solid solution strength), but the other undesirable effects of calcium remain.

It is obvious that alternative lead alloys for storage battery application would be most desirable. Unfortunately, development of lead alloys has been largely empirical over the years, and changes have been sluggish. The empirical nature is understandable in view of the difficulty of approximating service conditions in even the best-designed laboratory programmes. With this limitation in mind, the present study is intended to outline the approaches available for meeting specific requirements (for storage battery application of lead alloys) through microstructural control. Presently-used alloys and several new systems are examined from the standpoint of useful composition ranges, strengthening mechanisms, and corrosion properties. The fundamental reasons for the advantages and disadvantages of various alloy systems are evaluated.

1.1. Typical lead alloy development goals

It is customary in any alloy development programme to compile a list of desirable features prior to the experimental effort, and to rank these goals in some order of importance. In the case of lead alloys for storage battery grids, some

*Formerly Senior Scientist, ESB Inc, Carl F. Norberg Research Centre, Yardley, Pennsylvania, USA.

of these goals emerge as performance goals for the alloys themselves; others relate to desired methods in the design and processing of grids from a given alloy. These two kinds of goals cannot easily be separated. Typical goals are listed in Table I, in approximate order of decreasing concern.

TABLE I Lead grid alloy development goals

Mechanical strength
Corrosion resistance (penetration, weight loss)
Electrochemical "cleanliness" (antimony-free)
Character of corrosion product (lack of passivation)
Compatibility with active material (adherence)
Mechanical containment of active material (grid design)
Castability (if cast)
Weldability
Cost (alloying elements; methods of manufacture)

Strength is required in lead battery alloys for two distinct reasons. Sufficient grid stiffness is required for efficient processing of grids through automatic pasting machines and other handling equipment. Subsequently, the load-carrying members of the grid must resist creep-type (corrosion-assisted) deformation during service.

Corrosion products of the grid alloy are important from several standpoints. The corrosion resistance *per se* is of paramount importance, and includes a concern for the mode and extent of attack; for example, whether attack is general or concentrated at grain boundaries. The former situation is preferred to give a uniform corroded surface, as intergranular attack leads to grain separation, and contributes unfavourably to dimensional "growth" of the electrode in service. The character of the corrosion product is also important from the standpoint of electrochemical passivation and compatibility with other components of the battery electrode, particularly the "paste" (active material), the latter problem being primarily one of adherence. Certain corrosion products have "valve" or insulating properties with respect to passage of electrical current (i.e. will pass current in one direction but not the other, or will not pass current at all); this is, of course, not satisfactory in cells intended for cyclic service.

From a microstructural standpoint, strength and corrosion resistance do not always compliment one another. This is the general dilemma which is faced in evaluating new alloys, and which makes the development of strength superfluous without simultaneous consideration of corrosion, and vice versa. The most familiar battery grid failure mode is that of grid "growth", a phenomenon involving swelling and change of shape reminiscent of uranium alloys in reactors. This action is clearly a "conjoint" process, that is, requiring both mechanical stress and chemical or electrochemical contributions; classical creep studies must be considered carefully for relevance.

1.2. Brief history of lead alloy development

It is clear that historically, limited sophistication has been involved in lead alloy development work, with heavy dependence on empirical observations, past experience, and tradition. In fact, the alloys used in lead-acid battery systems have varied remarkably little over the years in spite of wide-ranging experimentation with new compositions.

The general, empirically-determined rationale for the usage of common alloying elements (Sb, Ca, Sn), and their shortcomings has been mentioned. In addition to these elements, there is fairly common usage of As (0.01 to 0.5%), particularly in standard antimonal alloys, and in Pb–Ca–Sn alloys. Arsenic is found to refine the eutectic microstructures in Pb–Sb alloys, enhancing castability, and causing more uniform corrosion [16-18]. It also increases the rate and amount of age-hardening in Pb–Ca alloys. However, As has a significant non-metallurgical disadvantage in that it is regarded as a health hazard and, therefore, incompatible with present pyrometallurgical techniques.

Numerous other alloying additions have been empirically investigated, with the primary aim of increasing corrosion resistance. A large number of elements, usually added in quite small amounts, have been reported to have a positive effect on one or more desirable features under some particular circumstances. Few of these elements have found their way into commerical compositions. The approximate composition ranges and effects reported for various elements are summarized in Table II. The most comprehensive survey of alloying effects remains the Armour Research Foundation work [19] of the late 1950s.

It cannot be overemphasized that any study of lead alloys for storage battery application requires extreme care to approximate or be able to accurately model or predict service conditions when fabricating and examining laboratory-scale samples. When examining the literature on

TABLE II Effects of alloying lead for storage batteries

Alloying element	Concentration range, (wt %)	Strengthening mechanism	Other positive effects	Negative effects	Recent references
Sb	5–12	Eutectic dispersion	Castability	Gassing Cost	[20-24]
Ca	0.05–0.09	Precipitation	Low gassing Low sulphation	Poor castability Refined grain size Reduced creep strength Passivating corrosion film	[8-14]
As	0.01–0.5		Refined eutectic microstructure Enhanced castability More uniform corrosion	Health hazard	[16-18]
Sn	0.02–5	Solid solution	Prevents passivation		[16, 25, 26]
Zn	1.5	Dispersion	Active material adherence	Selective leaching	[27]
Li	<0.03				[28, 29]
Cu, Ag, Cd, Tl, Hg	Small amounts		Reduced corrosion rate	Cost	
Rare earths	Small amounts		Grain refinement	Cost	
Cu	0.05–0.08				[24, 30]
Cd	≈ 0.03				[27, 31, 32]
Ag	0.05–0.4				[33-35]
Se	0.04–0.1				
Tl	0.7–2				[34, 35]
Te	0.03–0.8				
Al	0.01–0.1				
Ba	0.005–0.05				[27]

Note: In addition to the specific references cited here, a number of recent reviews dealing with alloying effects are available [9, 19, 22, 23, 27, 36-39].

the subject, it is clear that there has been widespread generation of data with limited relevance, due to overlooking this point. There has, in fact, been a historical failure of laboratory testing schemes to accurately predict service behaviour of battery alloys due to ill-designed and poorly characterized experiments. In general, the employment of high purity materials, usually an admirable procedure in basic physical metallurgy research, has led to difficulties in correlating laboratory results with in-service behaviour. This also applies prominently to discrepancies between laboratory and production fabrication procedures.

Of course, this dilemma is not unique to lead grid alloy systems. However, the unfortunate result in this case has been rather extensive, yet understandable, application of empirical techniques in the evaluation of new alloys. This is unfortunate because it becomes difficult to make fundamental determinations of strengthening mechanisms and the basic parameters governing them, as well as the fundamental parameters relevant to other properties. If such parameters were better isolated, property-property correlations could be made on considerably more sound bases. Also, while it is unlikely that battery service tests will be discarded as the ultimate evaluation for lead storage battery alloys, it has historically been seen that any metallurgical study related to the development of mechanical and microstructural features in lead alloys is unlikely to gain acceptance until the associated corrosion and electrochemical features are determined. This is also due in large part to the aforementioned lack of available basic correlations.

The present review will later endeavour to evaluate some of these fundamental parameters insomuch as is possible. This discussion will be introduced by a presentation of microstructural features in the classical alloy systems, and the

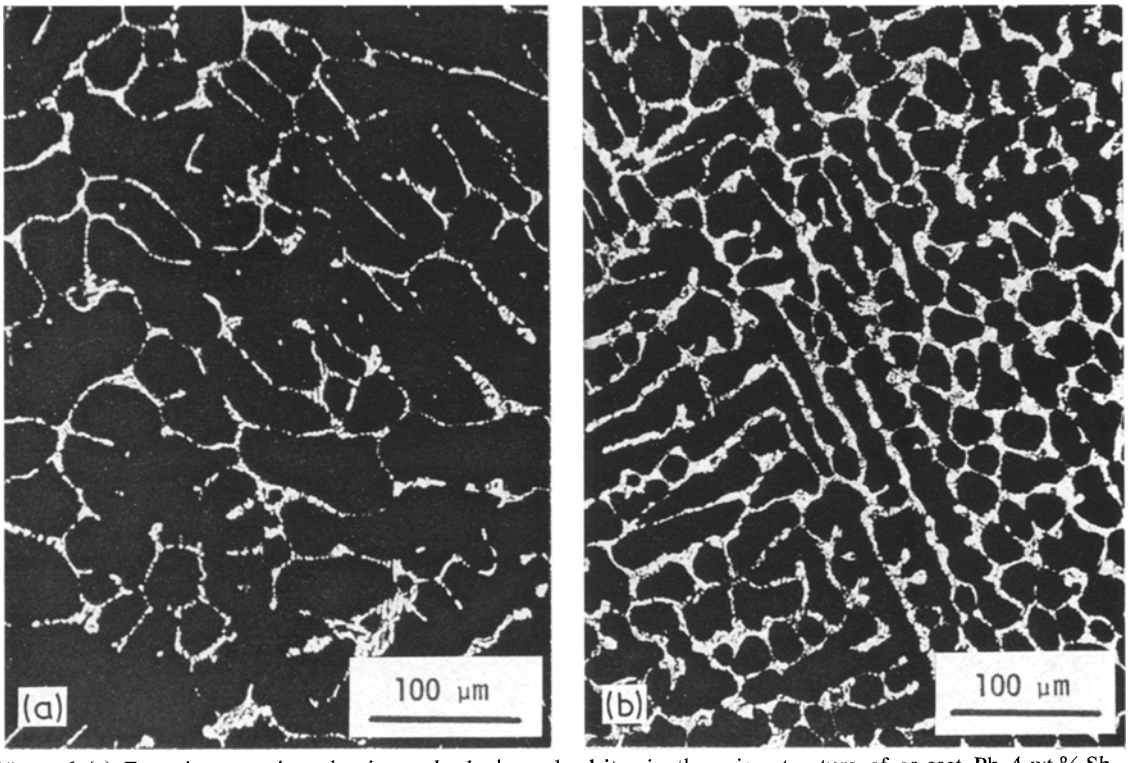

Figure 1 (a) Eutectic network and primary lead phase dendrites in the microstructure of as-cast Pb–4 wt % Sb alloy. (b) Refinement of the microstructure by increasing the Sb content, Pb–8 wt % Sb alloy. Polarized light photomicrographs. (Courtesy of VARTA Batterie AG.)

rationale for their development and utilization.

2. Classical methods of microstructural control

2.1. Alloying: the classical systems

2.1.1. Lead-antimony based alloys

Antimony is alloyed with lead in amounts typically ranging from 4 to 10 wt % Sb in battery alloys. With the Pb–Sb eutectic point at 11.1 wt % Sb, this produces a microstructure consisting of a eutectic network within dendrites of primary Pb solid solution (see Fig. 1). The primary purpose of Sb additions is to produce strength in terms of solid solution strength in the Pb-rich phase, and via the dispersion effect of a finely divided eutectic mixture. The latter feature also yields favourable corrosion uniformity in battery service, leading to gradual "wearing away" of the grids, instead of earlier failure due to localized attack. The microstructure can be somewhat refined by increasing the antimony content as displayed in Fig. 1. The strength of alloys leading to such microstructures can be modified significantly by varying the cooling rate from the melt. If the cooling rate is so rapid as to cause the phase compositions to lag behind the equilibrium values, an increase in strength will subsequently be noticed at room temperature, and the maximum hardness attained is greater than that attainable by slow cooling. This natural ageing phenomenon is very rapid with the major fraction of the total strength increase being demonstrated quickly (within a minute or so) and a minor increase occurring over a period of weeks. As will be discussed later, the microstructure can also be refined by more rapid cooling and the increased dispersion effect accounts for greater strength.

Pb–Sb binary alloys are commonly modified by relatively minor additions of other alloying elements, most often Sn and As. Tin is generally considered to add a favourable solid solution strengthening effect, and perhaps to play some favourable electrochemical role [9, 23, 25, 27, 36]. Arsenic refines the typical Pb–Sb network

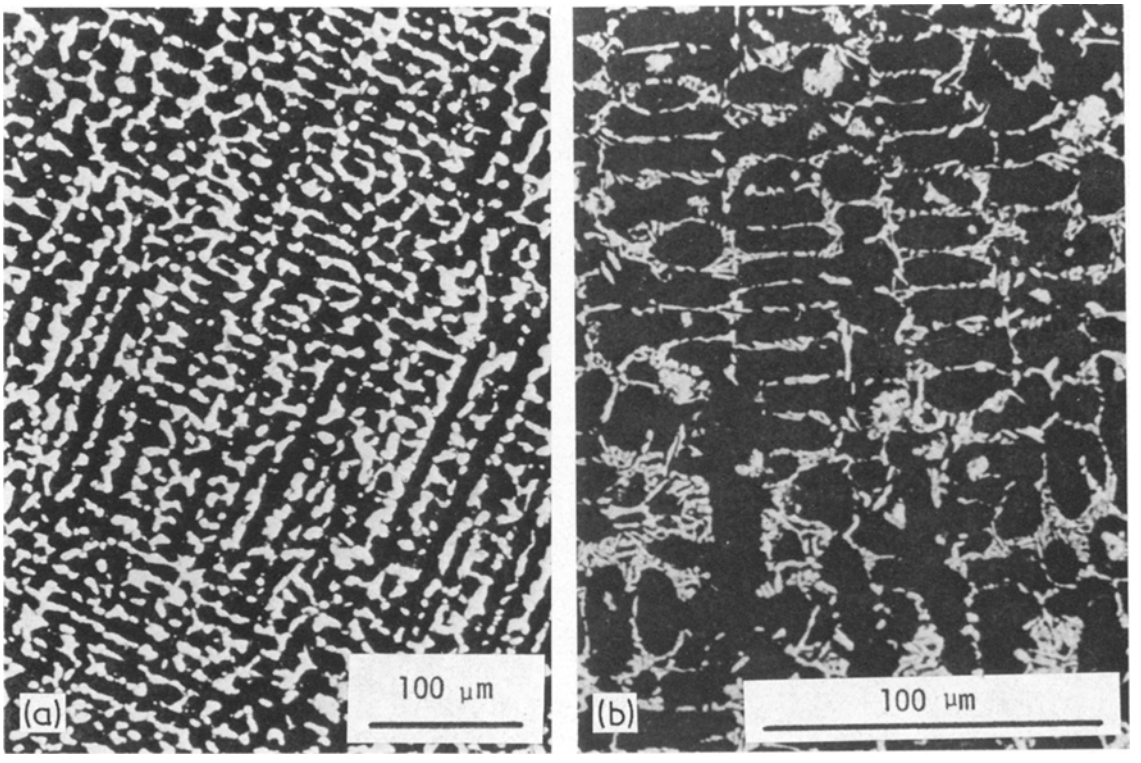

Figure 2 Microstructure of contemporary antimonal lead-acid storage battery grid alloy, Pb–6 wt % Sb–0.5 wt % Sn–0.5 wt % As. (a) × 200 (b) × 450. Primary lead solid solution dendrites surrounded by eutectic network. Polarized light photomicrographs. (Courtesy of T. W. Caldwell, NL Industries.)

eutectic microstructure, enhancing castability and promoting increased uniformity in corrosion [18]. Arsenic also increases the rate and quantity of the "age-hardening" strength increase subsequent to cooling to room temperature [17, 18]. The typical contemporary antimonal lead-alloy for lead-acid storage battery application (automotive) is approximately Pb–4.5 wt % Sb–0.5 wt % Sn–0.2 wt % As. A typical microstructure is represented by Fig. 2.

2.1.2. Lead-calcium based alloys

Lead-calcium alloys represent a classical precipitation-hardening binary system, with the maximum solubility of Ca in Pb being 0.10 wt % at the peritectic temperature of 328°C and diminishing to 0.01 wt % at room temperature. Storage battery alloys usually contain less than 0.08 wt % Ca, in order to minimize corrosion "growth" phenomena due to the grain refining effect of Ca. The typical microstructure of a Pb–Ca storage battery alloy, therefore, consists of essentially pure lead grains with a dispersion of Pb_3Ca particles, the amount and distribution (size, shape, and spacing) depending on alloy content and cooling rate (casting procedure) as for any age-hardening system. The Pb–Ca age-hardening response occurs "naturally," i.e. proceeds at room temperature in an alloy rapidly cooled from the melt (often referred to as a "quenched" alloy). This ageing can be and is sometimes effectively accelerated by artificial ageing (increasing the temperature above room temperature) a procedure not practical or necessary for the rapid Pb–Sb "ageing". The Pb_3Ca precipitate particles are generally too small to be resolved by light microscopy. Fig. 3 exhibits typical Pb–Ca microstructures wherein the presence of the dispersed phase is noticed indirectly by the irregular grain shapes.

The average grain size of such a microstructure can be reduced dramatically by increasing the Ca content (see Fig. 3). While an increase in Ca is very favourable strengthwise (primarily due to the effect on Pb_3Ca precipitation), the accompanying reduction in grain size is a serious

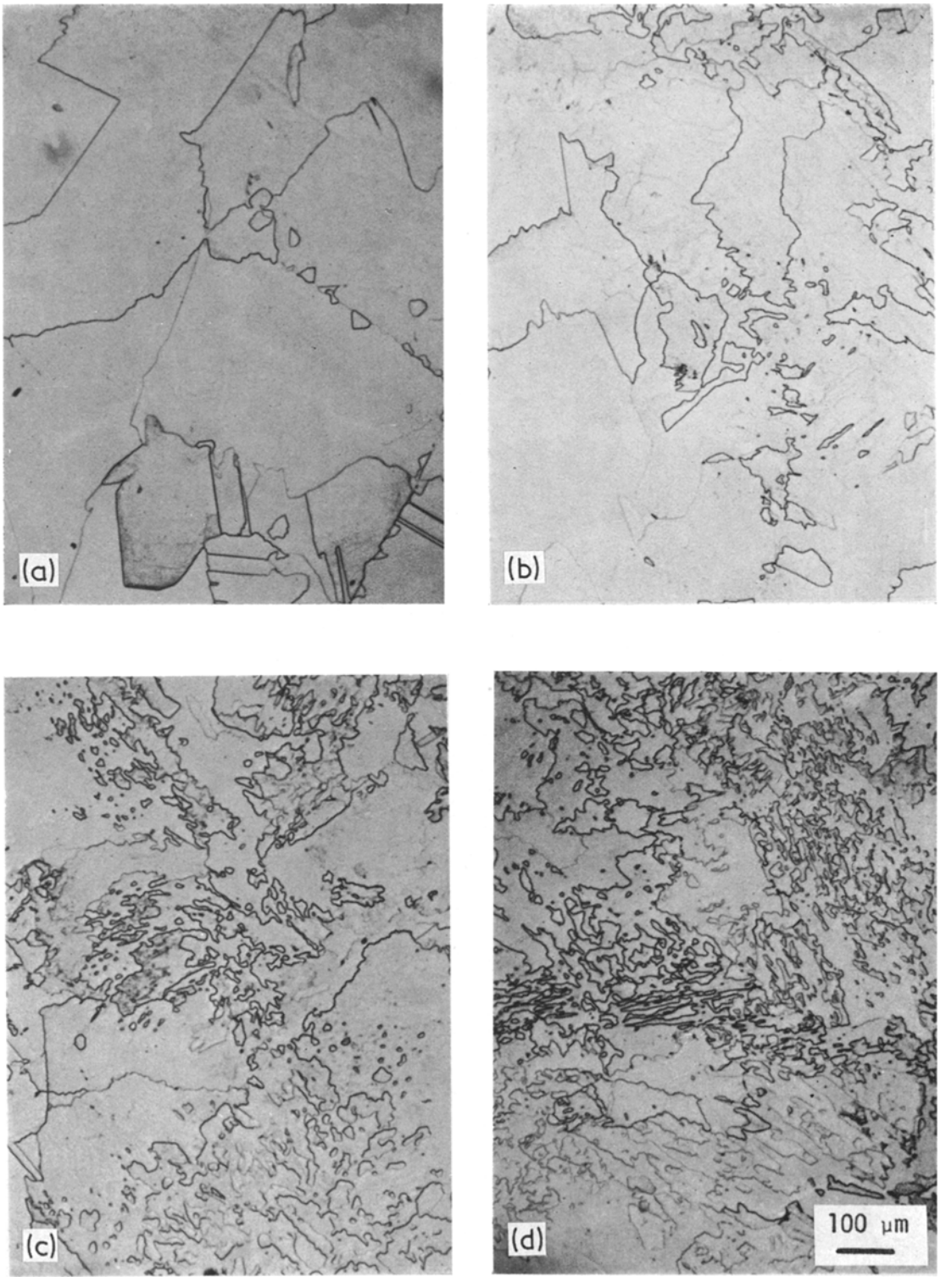

Figure 3 Grain refinement with increasing alloy content in as-cast Pb–Ca binary alloys (a) 0.05 wt % Ca (b) 0.06 wt % Ca (c) 0.07 wt % Ca (d) 0.09 wt % Ca. All at × 90.

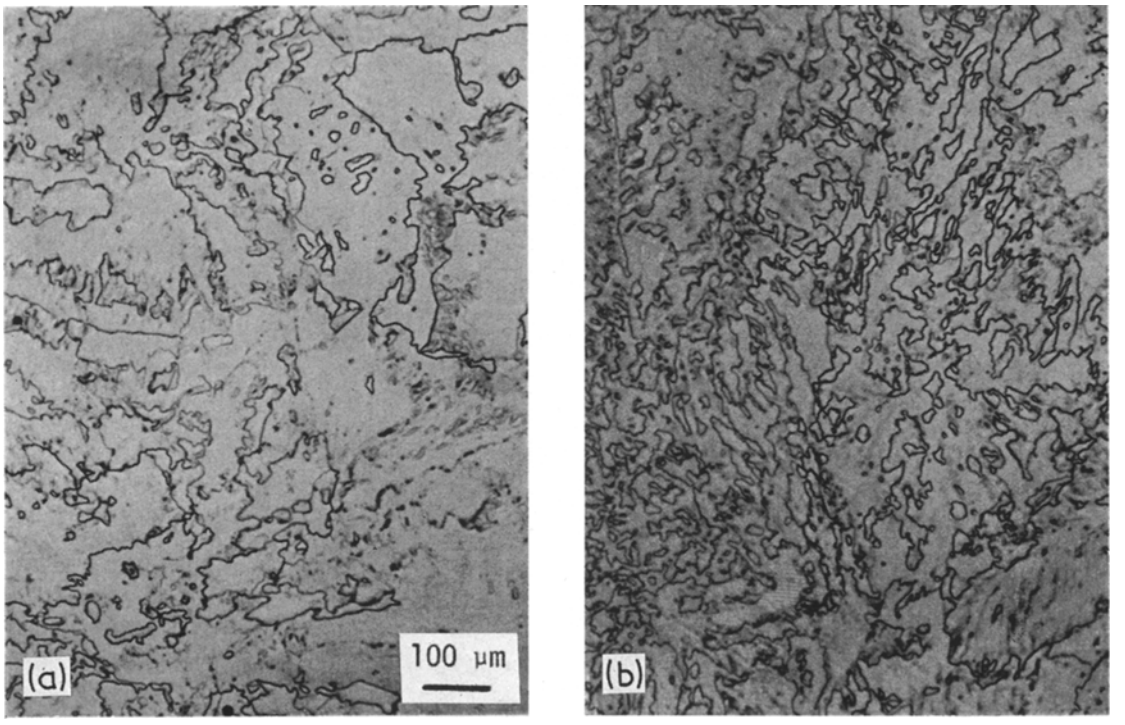

Figure 4 Contemporary lead calcium storage battery grid alloys contain tin below its solubility limit. These tin additions generally lend little microstructural distinction (a) Pb–0.08 wt % Ca (b) Pb–0.08 wt % Ca–0.5 wt % Sn. Both × 90.

detriment in terms of localized grain-boundary corrosion attack which prevails in these alloys. It is likely that grain-boundary enhanced precipitation promotes this attack, similar to the intergranular corrosion effect familiar in heat-treatable aluminium alloys. It is also clear that there is a pronounced corrosion product swelling effect (commonly referred to in these alloys as "exfoliation" or "shedding") [9, 10, 40] that leads to apparent "growth" of the storage battery grids in service (typically both the horizontal and vertical dimensions of a grid increase). Rapid cooling or pressure casting also unfavourably promote finer grain size in the lead-calcium based systems.

Tin is commonly added within its solubility limit to Pb–Ca alloys. This is primarily for electrochemical reasons as there is an apparent improvement in the character (physical properties) of the corrosion product. Tin lends little microstructural distinction (see Fig. 4). although contributing solid solution strength, particularly to the matrix Pb-rich phase. The typical contemporary calcium-lead alloy for lead-acid storage battery application (telephone and submarine batteries) is approximately Pb–0.07 wt % Ca–1.5 wt % Sn (see Fig. 5).

2.2. Casting techniques

Several methods can be used at the casting step in order to control the microstructure of lead storage battery alloys. Most of these methods operate by exercising some control of cooling rate from the melt. For example, simple changes in such parameters as melt temperature (superheat), mould temperature, and mould retention time have been commonly used over the years to control grain size and second phase dispersion; the storage battery industry has historically used large steel book moulds to cast grids, with melt superheat typically 300 to 600°F, mould temperatures approximately several hundred °F, and retention times of the order of less than a minute. Fig. 6 contrasts the microstructures formed by two different cooling rates (mould temperatures) in gravity casting of an antimonal lead storage battery alloy.

Recently, several more sophisticated tech-

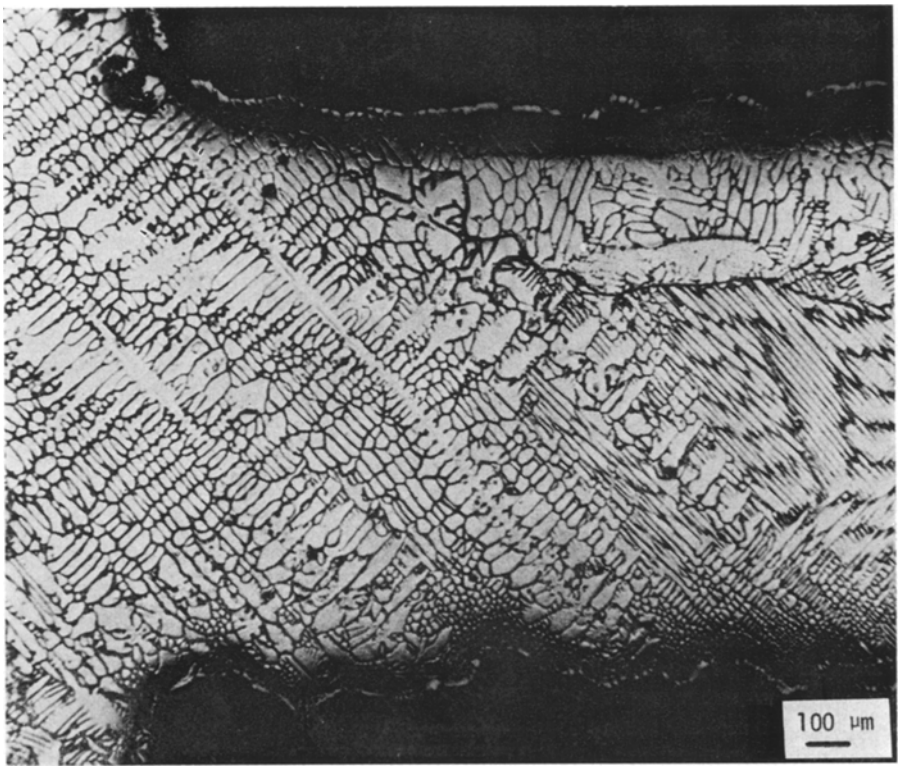

Figure 5 Cross-section of as-cast lead acid storage battery grid, Pb–0.075 wt % Ca–1.0 wt % Sn alloy. (Courtesy of T. W. Caldwell, NL Industries.)

niques have been applied, such as directional solidification and pressure casting. The general effects of such methods on solidification processes, and on nucleation and growth phenomena, are well known and will not be described in detail here. These techniques have the potential to control both grain size and shape, and in many cases drastically change the form and nature of lead storage battery alloy microstructures. While in practice, such techniques will be applied to alloys, it is revealing to observe the dramatic effect on the simple grain microstructure of pure lead (Fig. 7). Fig. 8 reveals the transverse and longitudinal sections of directionally solidified pure lead; Fig. 9 shows a similar effect in a dilute Pb–Sn binary alloy. It is clear that one of the results possible with directional solidification techniques is a variation in microstructure similar to that typical of wrought metals. Degrees of these directional effects are commonly produced unintentionally in cast alloys, which can be seen in Fig. 5 for example.

The primary effect of pressure casting is a substantial refinement of microstructure which can be appreciated by comparing the structure of the gravity cast antimonal alloys in Figs. 1 and 6 with the pressure cast alloy of Fig. 10.

3. Microstructure-mechanical properties relationships

A primary goal of this review is to investigate the applicability of contemporary metallurgical techniques to the control of microstructure and, consequently, mechanical strength, in lead alloys utilized as battery grids. It is, therefore, appropriate to present a brief review of the pertinent microstructural parameters affecting mechanical behaviour of such alloys. It is especially relevant to note that ambient temperature for lead grid alloys is approximately half the melting temperature (T_m) of pure lead on the absolute scale, so that service temperatures for grid alloys can range from 0.5 T_m to 0.7 T_m for the particular alloy. Such temperatures are sufficient to allow significant additional degrees of freedom to

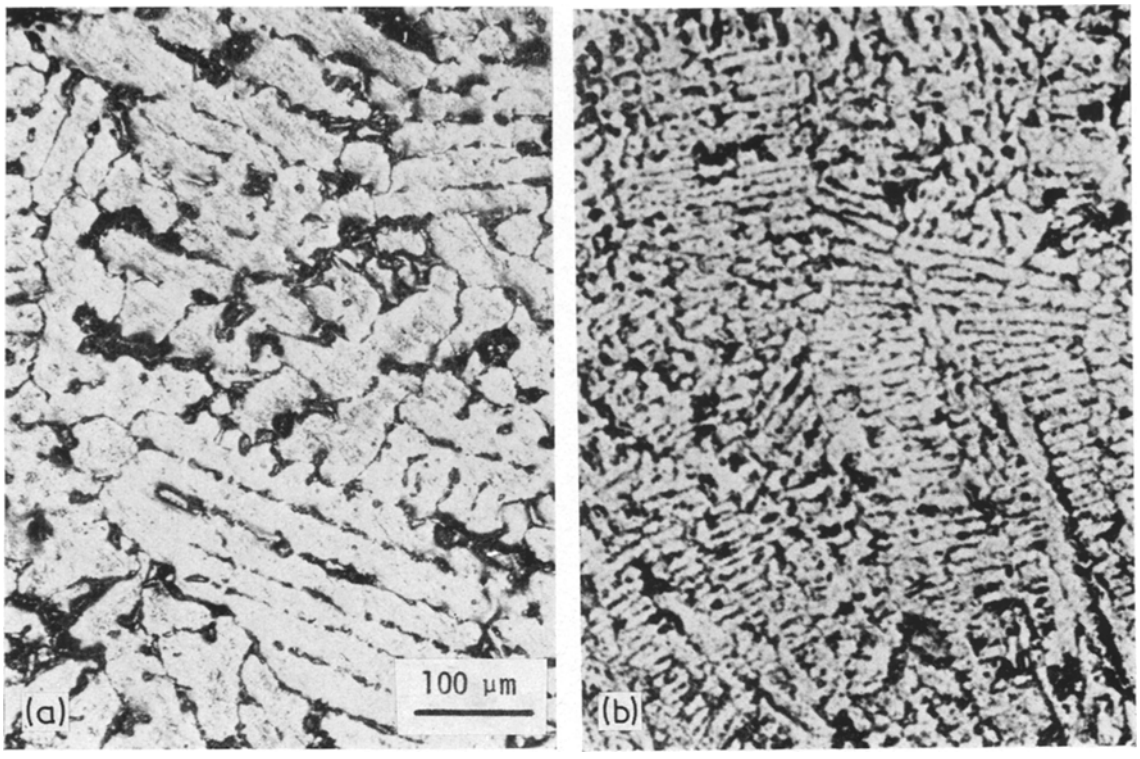

Figure 6 Effect of cooling rate during solidification of antimonal lead alloys. (a) Pb–4.5 wt % Sb–0.4 wt % Sn–0.2 wt % As–0.05 wt % Cu, slowly solidified; (b) same alloy, more rapidly solidified, shows microstructural refinement. Both × 160. (Courtesy of St. Joe Minerals Corporation.)

Figure 7 Equiaxed grain structure of (conventional) gravity cast pure lead (Courtesy of VARTA Batterie AG.)

dislocations which would otherwise be substantially immobilized by various microstructural barriers (such as solute atoms, second phase particles, or other dislocations) at 0.4 T_m and below. A discussion of mechanical strength in lead alloys in service appropriately becomes one of creep behaviour. Similarly, deformation involved in handling grids during fabrication is most accurately considered a competition between dislocation-generation (strain-hardening) processes and dislocation-annihilation (recovery) processes.

When initially stressed at a temperature greater than approximately 0.4 T_m, a metal strains at a rate which uniformly decreases to a constant value, the steady-state creep rate. Although primary creep may be appreciable ($\approx$ 10 % true strain), creep studies have tended to focus on determining the steady-state creep rate to simplify experimentation. Fortunately, significant evidence exists that primary and secondary creep display the same stress dependence [41] so that

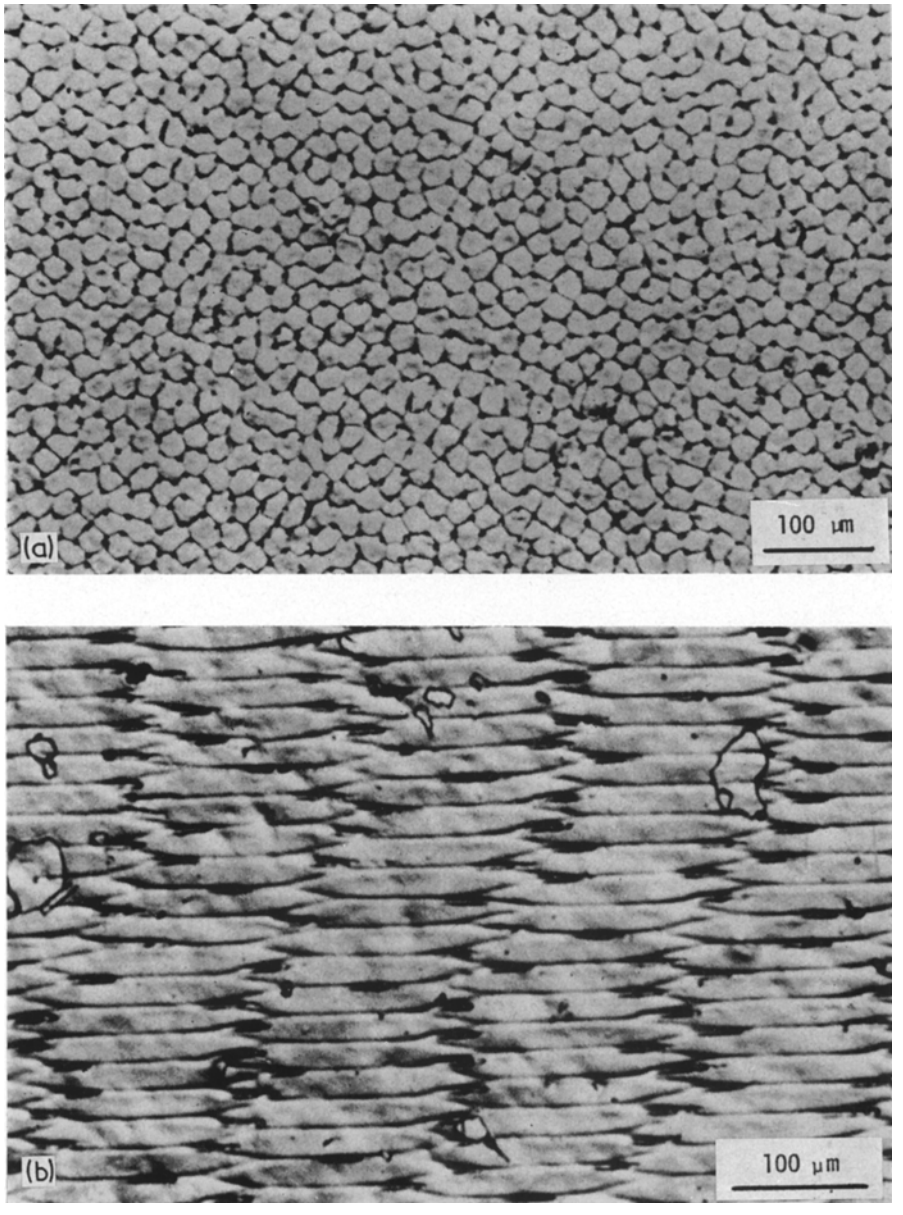

Figure 8 Grain shape effect of directional solidification of pure lead. (a) transverse section; (b) longitudinal section. (Courtesy of T. W. Caldwell, NL Industries.)

it may be assumed that a microstructural parameter which reduces the steady-state creep rate, at a given temperature and stress, would improve the creep resistance in general.

3.1. Stress and temperature dependence

It is generally accepted that for metals the stress dependence of the steady-state creep rate depends on both temperature and stress. The equation usually proposed to describe high temperature creep behaviour of metals is of the form:

$$\dot{\epsilon}_s = K\sigma^n \, e^{-Q_c/RT} \qquad (1)$$

where $\dot{\epsilon}_s$ = steady state creep rate, K = material constant, σ = flow stress, n = stress exponent,

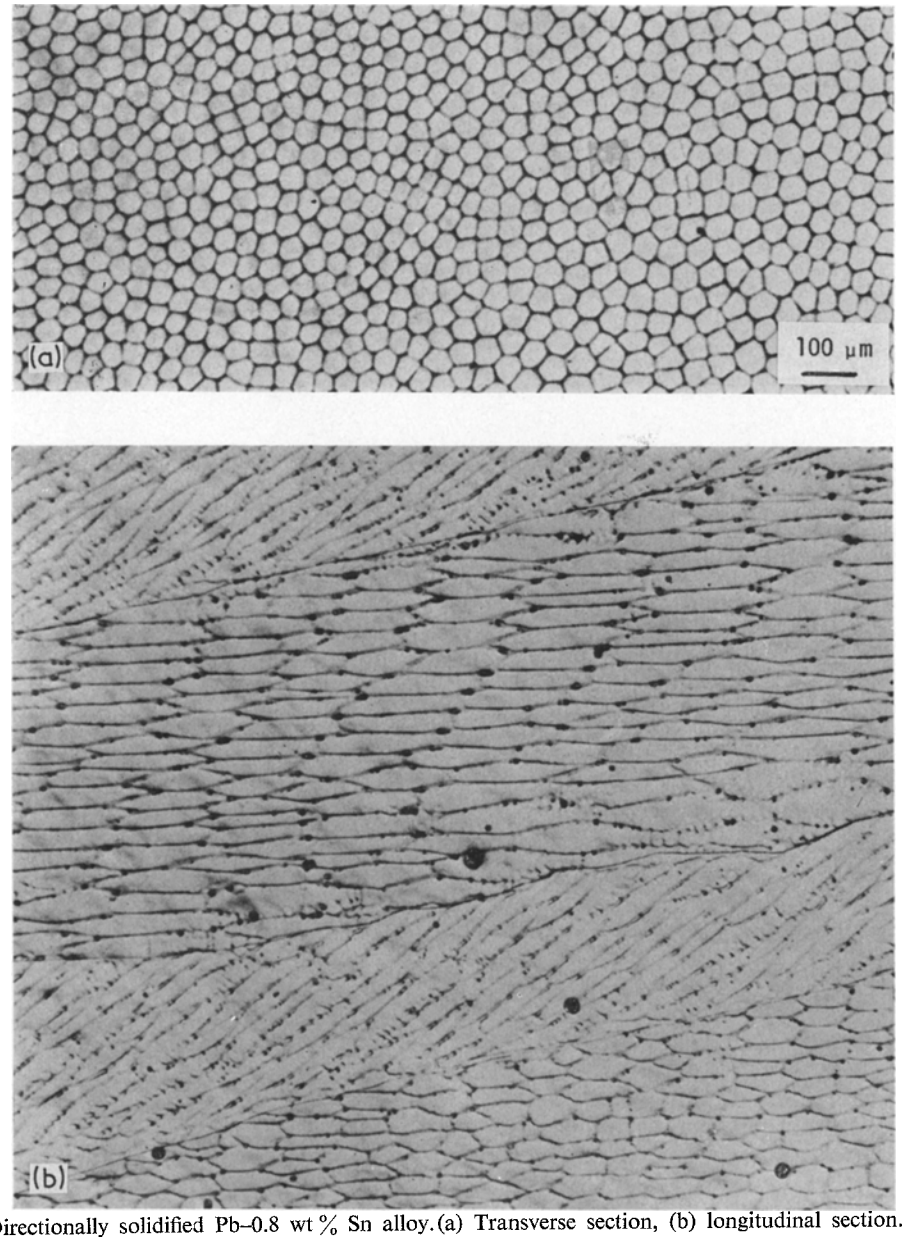

Figure 9 Directionally solidified Pb–0.8 wt % Sn alloy. (a) Transverse section, (b) longitudinal section. (Courtesy of T. W. Caldwell, NL Industries.)

Q_c = creep activation energy, R = gas constant, and T = absolute temperature. The creep activation energy, Q_c, has been shown to be equal to the self-diffusion activation energy, $Q_{s.d.}$, for many pure metals [42]. Creep behaviour over a wide range of stresses and temperatures can thus be examined by plotting diffusion-compensated strain-rate versus stress to obtain a single-valued function:

$$\frac{\dot{\epsilon}_s}{D_0 e^{-Q_c/RT}} = \frac{\dot{\epsilon}_s}{D} = \frac{K}{D_0}\sigma^n = A\sigma^n . \quad (2)$$

Here D_0 = the self-diffusion pre-exponential factor, D = self-diffusivity, and A = a material constant containing some structural parameters we might hope to alter. Such an overall correla-

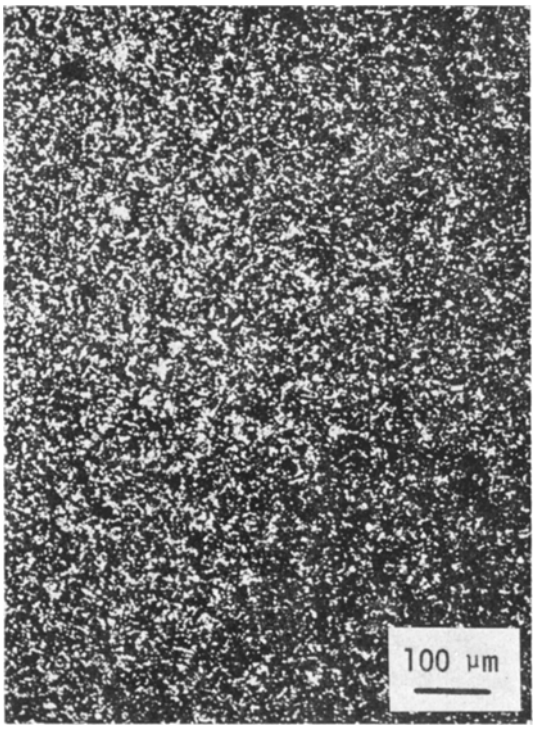

Figure 10 Extreme microstructural refinement in pressure cast Pb–9 wt% Sb alloy. Polarized light photomicrographs. (Courtesy of VARTA Batterie AG.)

tion, originally presented by Sherby and Burke [42], is shown schematically in Fig. 11. At low stresses and high temperatures, strain-rate is linearly dependent on stress (region I). Here Creep occurs by mass transport independent of dislocation motion (so-called Nabarro-Herring creep) and is of minor interest here. Region II can be represented by:

$$\frac{\dot{\epsilon}_s}{D} = A\sigma^5 . \qquad (3)$$

Creep resistance in region II is generally considered to be controlled by the rate at which immobilized dislocations can escape their barriers by climb. Region III displays an even greater sensitivity of strain-rate to stress; here dislocation climb, enhanced by excess vacancies generated at the high strain-rates and low temperatures, has been considered the controlling phenomenon.

Regions II and III are the environments in which lead alloys exist during fabrication and service. Therefore, mechanical strength improvement must be concerned not only with immobilizing dislocations, but with preventing the occurrence of relaxation mechanisms such as dislocation climb or grain-boundary sliding (also controlled by diffusion).

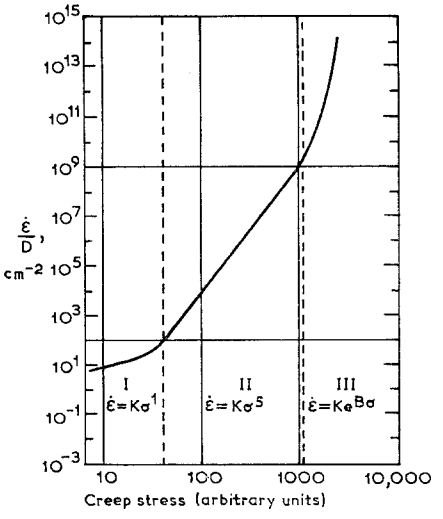

Figure 11 The stress dependence of the diffusion-compensated steady-state creep rate for a typical pure polycrystalline metal (Courtesy of Sherby and Burke [42].)

3.2. Microstructural parameters

3.2.1. Solid solutions

Experimenters have quantified the effects of diffusivity (D), elastic modulus (E), and stacking fault energy (γ) on the steady-state creep rate, $\dot{\epsilon}_s$, of pure metals [42], as

$$\dot{\epsilon}_s = A' D\gamma^{3.5}(\sigma/E)^5 . \qquad (4)$$

Equation 4 indicates that creep-resistance is enhanced by high modulus, low diffusivity, and low stacking fault energy. Each of these parameters can be altered by solid solution alloying; therefore, prediction of the effect of alloying on creep resistance fundamentally involves consideration of the effect of alloying on these parameters. This has been vividly illustrated by Sherby and Burke [42] in the case of Zn solutioned in Cu. In this example of a class of solid solutions, it has been shown (Fig. 12a) that additions of up to 10% Zn to Cu improve creep resistance, apparently because a decrease in stacking fault energy dominates. Greater Zn additions are not beneficial, apparently because an increase in diffusivity dominates. In contrast, Sherby and Burke [42] show that other solid solutions, exemplified by Au–Ni (Fig. 12b) exhibit creep resistances which follow the same

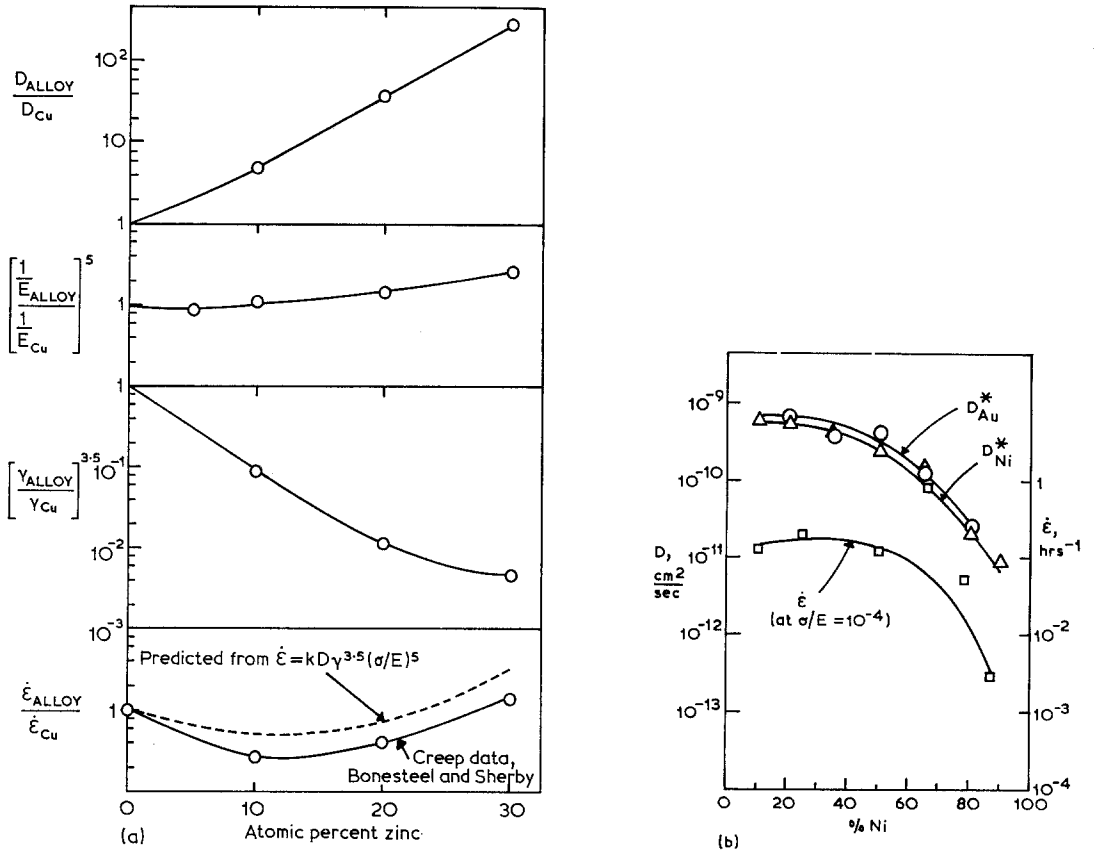

Figure 12 (a) Solid solution alloying in the Cu–Zn system; the influence of zinc on the creep behaviour of copper, explained by changes with alloying, in the diffusion rate, elastic modulus and stacking fault energy. (Courtesy of Sherby and Burke [42]). References indicated above are cited in [42]. (b) Solid solution alloying in the Au–Ni system; the influence of gold on the creep behaviour of nickel, explained by changes, with alloying, in the diffusion rate. (Courtesy of Sherby and Burke [42].)

trend as the diffusion coefficient, which suggests that in these cases, stacking fault energy and modulus are not as important as diffusivity. There is evidence that alloying can also affect creep strength when changes in γ, E and D are minor [43]. Solutes are known to interact with dislocations in several ways; the most prominently mentioned interactions usually are related to the elastic stress fields associated with the various types of lattice imperfection. Such interactions generally inhibit dislocation mobility, including those accommodations which allow recovery [44].

3.2.2. Grain size and subgrain size effects

The effect of grain size on creep strength is not clearly defined. The best evidence to date indicates that grain boundaries may have either a strengthening or weakening effect, depending on the stresses and temperatures to which the metal is subjected [41, 44]. If the environment corresponds to region III of Fig. 11, normal grain-size strengthening, i.e. increased creep strength with decreased grain size, would be expected. Exposure in region II could (but not always) produce the reverse effect; as enhanced atom mobility increases the contribution of grain-boundary sliding to the creep strain, small grain size could be detrimental to creep strength.

Subgrain structure may play an even more important role in determining creep resistance. Many materials develop a subgrain structure during extensive deformation at elevated temperature, with the subgrain size determined by

the stress (or the parameter $\dot{\epsilon}/D$ – see Fig. 11). The higher the creep stress, σ, the finer the subgrain size, λ, as $\sigma \sim \lambda^{-1}$ [42, 45-47]. Materials with low stacking fault energy show less tendency to develop subgrains, probably because of the reduced tendency for cross slip. Sherby and Burke [42] have shown that when pure aluminium was pre-crept at 4000 psi*, then crept at 2000 psi, the instantaneous creep rate was about ten times less than that for aluminium crept continuously at 2000 psi. This difference, attributed to a difference in subgrain size, disappeared with continued strain, as subgrains grew to the steady-state size compatible with 2000 psi. The possibility remains, however, that such substructures, developed by prior thermo-mechanical working, can be stabilized by treatments which preferentially leave solute atoms or second phase particles at the boundaries. The high-temperature strength could then be expected to be significantly improved; in fact, very recent studies indicate that subgrain strengthening may be one of the more significant methods of improving high-temperature properties [48].

Many authors [49-53] refer to the high-temperature strengthening resulting from a stabilized, three-dimensional "dislocation network" or a "polygonized dislocation substructure". We will not make the distinction here between that kind of dislocation substructure and a subgrain structure, but view the former as an imperfectly formed version of the latter. The perfection of a subgrain structure is a sensitive function of the deformation rate and the temperature at which it was formed; the most well-developed subgrains representative of a particular flow stress are obtained by a combination of high deformation rate and high temperature. This fact has important implications, for it is also true that the more perfectly developed the subgrain structure, the more effective is the subgrain boundary as a barrier to plastic flow [47, 48].

3.2.3. Second-phase particles

A very potent and proven method to increase mechanical strength at high temperatures is to introduce a fine dispersion of second phase particles. Classic examples are sintered aluminium powder (SAP) and thoria dispersed nickel (TD-nickel). Both systems have received considerable study, and there is general agreement that $\sim 3\%$ of finely dispersed particles (Al_2O_3 in Al, ThO_2 in Ni) make the respective metals ten to twenty times stronger at certain values of strain-rate and temperature. Reasons for this are poorly defined; however, it is clear that the matter cannot be viewed as simple Orowan bowing of mobile dislocations.

Current theories do not lend insight useful for technological control, although it is generally accepted that second phase particles should be relatively insoluble, small, stronger than the matrix, and closely and evenly spaced to provide optimum strengthening. The mechanism(s) underlying second phase creep strengthening are clearly related to a reduction in the ability of recovery phenomena to occur; hard particles stabilize grain boundaries (and reduce grain-boundary sliding) and promote retention of substructural features such as subgrain boundaries and dislocation tangles.

3.2.4. Other microstructural features

Some evidence exists to indicate that grain *shape* affects creep strength. Wilcox and Clauer [54] have shown that TD-nickel and TD-nickel-chromium alloys, processed to contain long, thin grains, were about ten times stronger (in a loading direction parallel to the length of the grains) than an equiaxed structure. Their conclusion was that grain-boundary sliding dominated the creep behaviour of these alloys, and that orienting the grain boundaries parallel to the applied stress minimized the fraction of boundary which could shear. Versnyder and Shank [55] reached similar conclusions after evaluating a directionally solidified nickel-base superalloy. These conclusions cannot yet be generally applied, however. For example, Embury *et al.* [56] concluded that the presence of an elongated subgrain structure had no effect on the creep behaviour at 450°C of a 7075 aluminium alloy.

4. Emerging methods of microstructural control

4.1. Dispersion strengthening

Dispersions of second phase particles in a lead or lead alloy matrix can be produced by several methods other than conventional casting or age-hardening schemes. The methods which will be discussed here are those in which the dispersoid is essentially insoluble in the solid lead alloy matrix. Such dispersions can be produced by: (i)

*10^3 psi = 6·89 N mm^{-2}

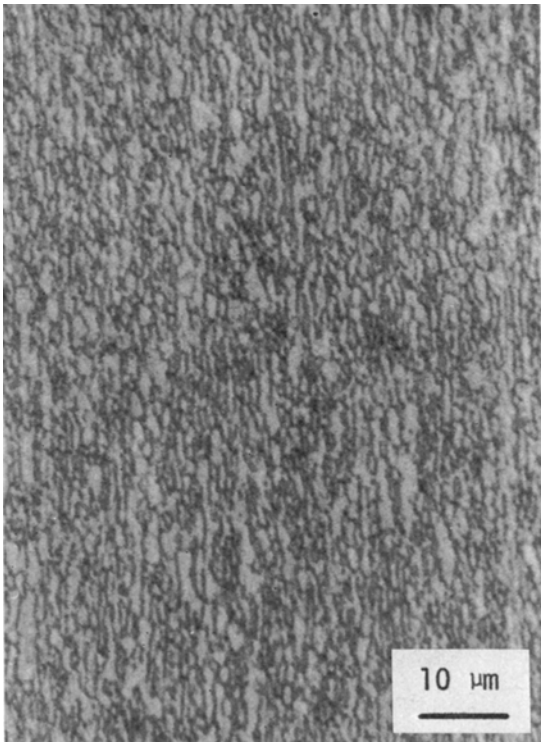

Figure 13 Microstructure of commercially developed dispersion-strengthened lead (PbO dispersoid), "St. Joe DS Lead" (Courtesy of St. Joe Minerals Corporation.)

powder metallurgy techniques; (ii) "shotting" of the melt; or (iii) formation of insoluble, "natural", dispersoids in the particular alloy system during solidification.

4.1.1. Powder metallurgy techniques

Dispersions of a number of insoluble materials in lead have been produced by powder metallurgical techniques. Specific dispersoids which have been investigated include lead oxide (PbO) most prominently [57-61] as well as Cu [61-63], Al [61-63], Cr [61], alumina (Al_2O_3) [61, 64, 65], Ni [66, 67], WC [68], and SiC [68]. Consistent with observations in other systems, sub-micron-sized dispersoids present as several percent are most effective. Little work has been done with lead alloy matrix materials. Materials with 1 to 5% lead oxide were recently developed nearly to the point of commercial availability in rolled, drawn, and extruded forms [58]; a high magnification photomicrograph of fine-grained "St. Joe DS Lead" is shown in Fig. 13.

Processing methods leading to dispersoids in lead can be quite different from those used for powder metallurgy materials involving higher temperature matrix mixtures. In the case of most such familiar metals, the dispersion is produced by intimate mixing of powders of both the parent metal or alloy and the insoluble second phase; the mixture is then compacted, sintered, and formed in the usual manner for a powder metallurgy product. In the case of lead-based materials, the procedures utilized have been somewhat more diverse and less restrictive. This advantage is gained because consolidation of lead or lead alloy matrix materials usually does not require application of external heat, so that more direct consolidation processes are possible.

For example, PbO dispersions can be produced simply by direct deformation of lead powder [59, 60, 69], with the PbO introduced via fragmentation and incorporation of the natural oxide film pre-existent on the lead particles; in some cases, formation of this oxide layer may be enhanced by moisturization or roasting procedures. (Lead and lead oxide powder of suitably small sizes are readily producible through the normal technology utilized in paint technology and lead-acid battery paste manufacture.) Alumina dispersions can be produced in similar fashion by mixing Pb and Al_2O_3 powders, with a reducing step introduced to remove PbO layers from the Pb particles [65, 70]. Alumina-lead mixtures have also been produced by means of a sequence consisting of aqueous co-precipitation of Pb and Al compounds, followed by roasting to oxides, and hydrogen reduction to directly form an intimate mixture of fine Pb and Al_2O_3 powders, which can then be pressed, extruded, etc. to produce solid aggregates containing several percent Al_2O_3 [64]. Metallic dispersions (Cu, Al, etc.) are more often produced by rapid freezing methods such as atomization [63] of alloys to produce mixed powders which subsequently may be compacted.

4.1.2. Solidification techniques

Dispersoids can also be formed by causing a phase insoluble in the solid state to be introduced prior to complete solidification of the melt. This phase may be introduced artificially by "shotting" of the melt, or may be natural to the particular alloy system (i.e., the product of the primary solidification reaction). The latter type of liquid state precipitates will be referred to here as natural dispersoids (distinct from natural

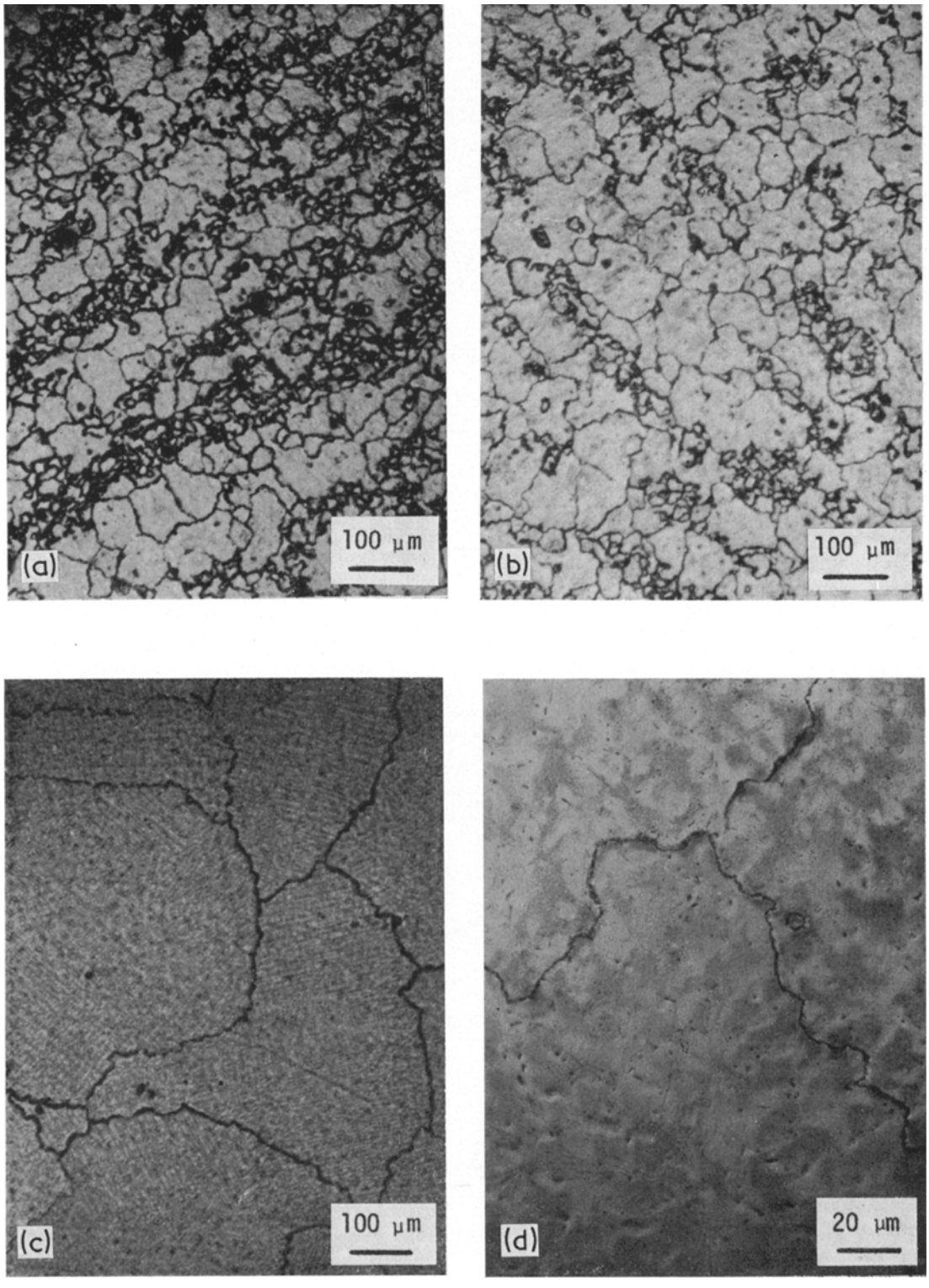

Figure 14

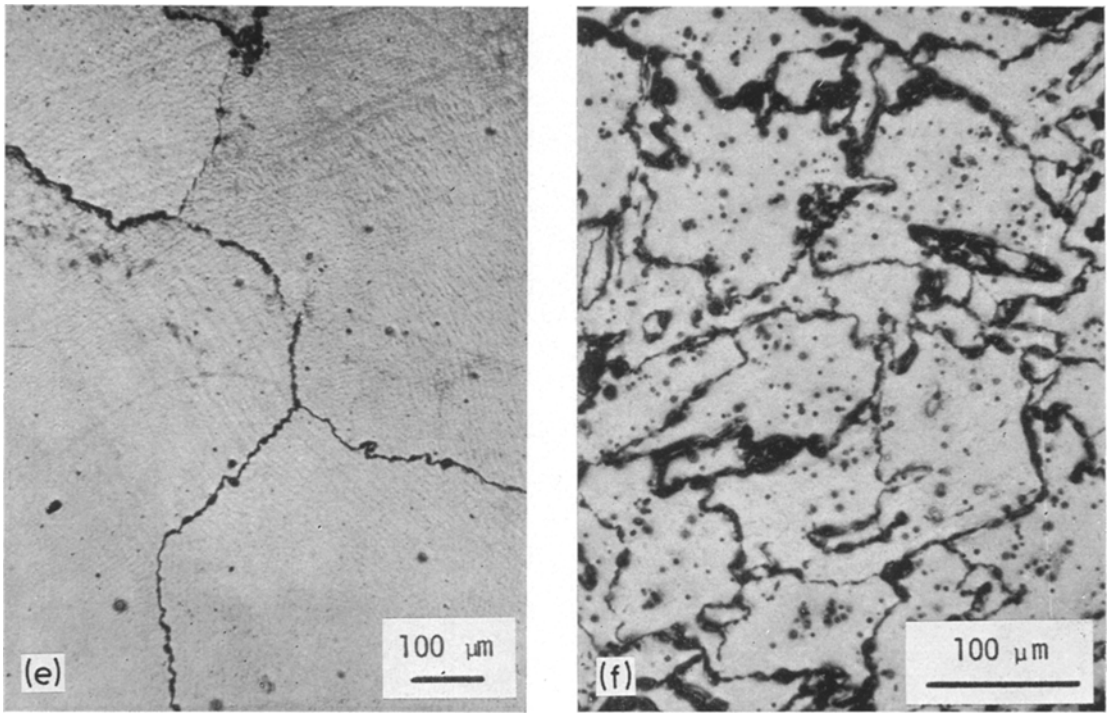

Figure 14 As-cast (slow-cooled, 1050°F liquid metal temperature, 450°F mould temperature) microstructures in Pb–Zn–Sn alloys. The primary zinc phase effectively provides *in-situ* "shotting" of the melt, resulting in refinement of the lead-tin (solid solution) grains with increasing zinc content, demonstrated by comparing (e) versus (d) versus (a) versus (f). (a) versus (b) demonstrates that tin content has little microstructural effect. (a) Pb–1.5 wt % Zn–1.5 wt % Sn, × 100. (b) Pb–1.5 wt % Zn–2.5 wt % Sn, × 100. (c) Pb–0.7 wt % Zn–1.5 wt % Sn × 100. Note the irregular grain-boundary conformation and fine precipitate structure within the grains. (d) Same as (c), × 500. (e) Pb–0.5 wt % Zn–0.5 wt % Sn, × 100. (f) Pb–2.3 wt % Zn–1.5 wt % Sn, × 200. Note the extremely irregular conformation of the grain boundaries.

solid state precipitates) and discussed separately.

Shotting of lead alloy melts with alloying elements is not an uncommon practice in lead pyrometallurgy. In order to reduce oxidation (drossing) losses, this is often done shortly before casting. If an insoluble element or compound is introduced to the melt as a fine powder, subsequent solidification will be effected, and the shotted substance also may become a part of the final stable microstructure. The insoluble "shotted" substance can, therefore, contribute both directly and indirectly to the final chemical and mechanical properties of the alloy.

A number of systems have been investigated in which a dispersoid is formed by natural precipitation from the melt. A prototype for such systems is that based on the insolubility of zinc in solid lead. Fig. 14 shows the conventional gravity cast microstructures for several Pb–Zn–Sn alloy compositions. Tin is present in these alloys below its solubility limit, and exhibits little microstructural influence. As the zinc content is varied, however, the nature and amount of primary dispersoid is changed, which influences nucleation during solidification of the lead-phase grains, and also grain shape due to grain-boundary pinning effects. It is clear that as the zinc content is increased, the average grain size decreases, and the grains become considerably more irregular in shape.

Thermomechanical working of such alloys demonstrates the effectiveness of grain-boundary pinning by natural dispersoids. Pure lead and many of its alloys will spontaneously recrystallize during and after room temperature deformation, destroying much of the strengthening effects of working. In storage batteries, the

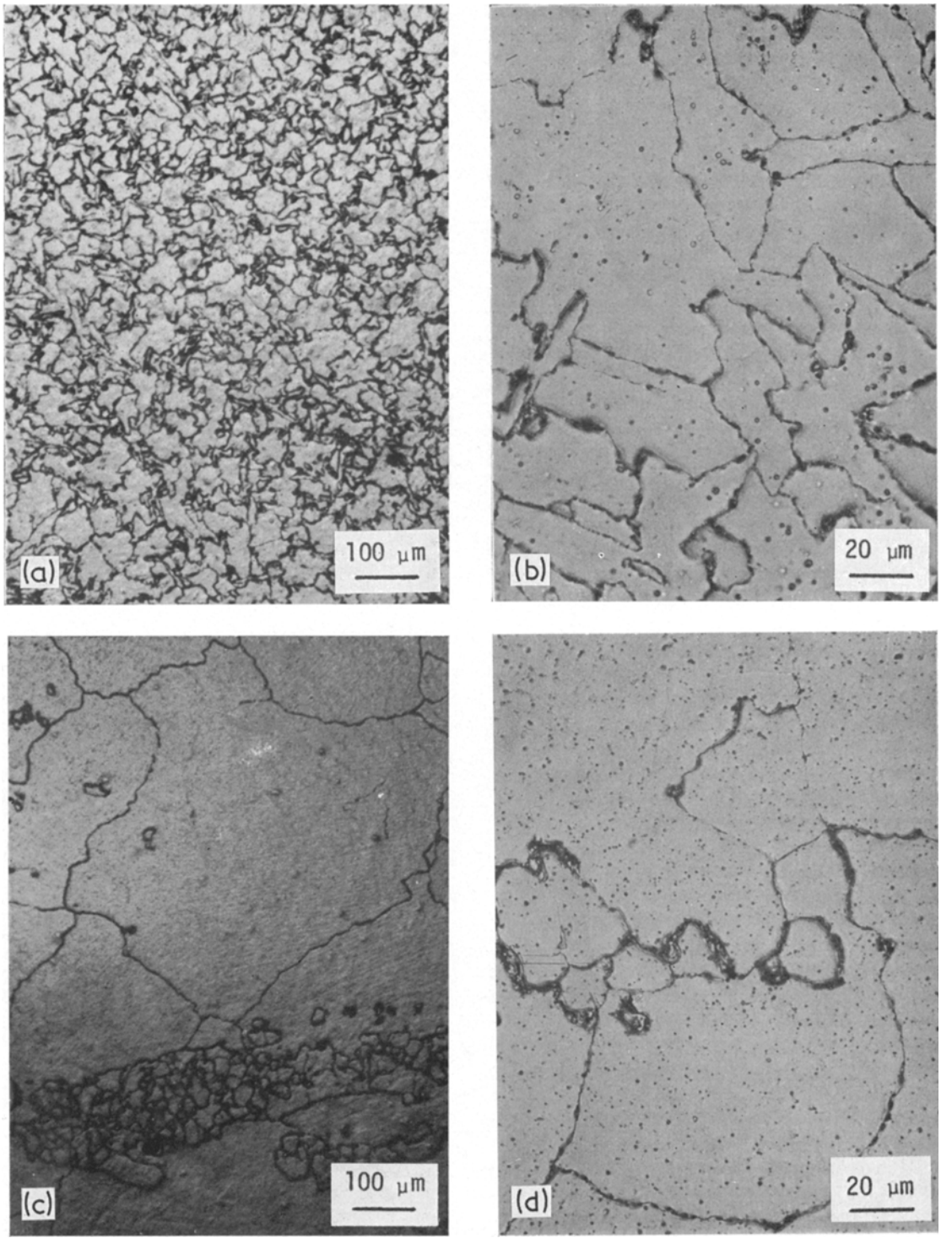

Figure 15 "Chill casting" (900°F liquid metal temperature, 300°F mould temperature) Pb–Zn–Sn alloys accentuates the grain refinement and grain-boundary pinning effects of the dispersed zinc primary phase. (a) Chill cast Pb–1.5 wt % Zn–1.5 wt % Sn × 100. Compare with the slow-cooled structure of Fig. 14a. (b) Same as (a), × 500. (c) Chill-cast Pb–0.7 wt % Zn–1.5 wt % Sn, × 100. (d) Same as (c), × 500.

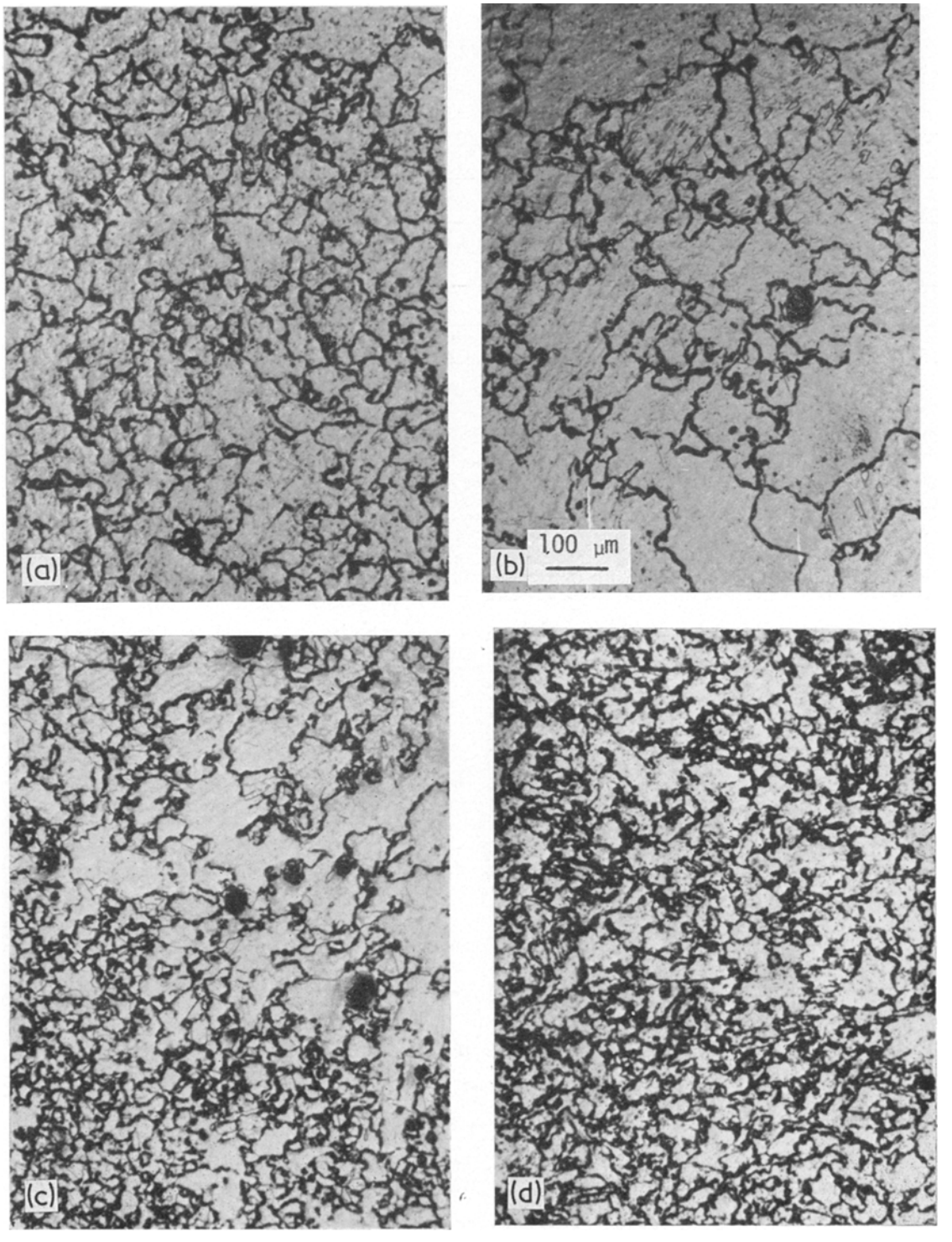

Figure 16 Deformed (40% reduction in thickness) and (room temperature) recrystallized Pb–Zn–Sn alloys (originally slow-cooled as Fig. 14). All × 100. (a) Deformed Pb–1.5 wt % Zn–2.5 wt % Sn. Compare with Fig. 14b. (b) Deformed Pb–0.7 wt % Zn–1.5 wt % Sn. Compare with Fig. 14c. (c) Deformed Pb–0.5 wt % Zn–0.5 wt % Sn. Compare with Fig. 14e. (d) Deformed Pb–2.3 wt % Zn–1.5 wt % Sn. Compare with Fig. 14f.

additional activation of recovery processes by high operating temperatures (perhaps up to 200°F in automotive service) promotes such softening. High service temperatures also accelerate conventional creep processes. Microstructural features which inhibit grain-boundary migration and/or sliding will be favourable with respect to both recrystallization and creep resistance. Insoluble precipitates have been shown to have this effect (see Fig. 16). The stability of the insoluble particles at operating temperatures is also very beneficial, in contrast to precipitates which may coarsen or dissolve, drastically changing properties as a function of time.

In another interesting system, Pb–Zn–Bi, dual microstructural control can be exercised through (i) the insolubility of zinc in solid lead, and (ii) the Pb–Bi–eutectic reaction. By varying the Zn and Bi content and cooling rate effects, much control can be exercised over microstructure and properties as seen in Fig. 17.

It should be noted that the electrochemical suitability of alloys containing zinc is unproved. It is known that zinc is insoluble in battery electrolytes, an obvious necessity; however, detailed knowledge of battery service behaviour is unknown. Zinc is by no means the only natural dispersoid which might be applied. Arsenic, barium, and silver, among others, have similar effects on grain size and shape due to grain-boundary pinning.

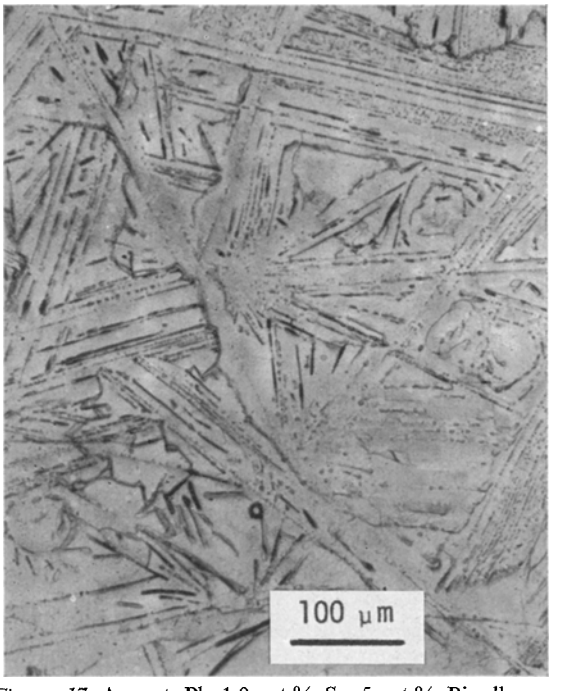

Figure 17 As-cast Pb–1.0 wt% Sn–5 wt% Bi alloy. × 150.

4.2. Thermomechanical processing

Lead alloy grids for storage batteries have been produced almost exclusively by casting, largely due to cost considerations. This limitation has diminished the possibility of introducing strength via the fabrication process, and has restricted compositions due to castability requirements. Also, in choosing between cast and wrought grids, the primary role of the grid, to mechanically contain active material, must be considered. Due to design and surface texture differences, the ability to effectively hold battery paste can vary widely depending upon the fabrication processes employed. However, the potential of wrought grids has stimulated increased exploration in recent years.

In attempting to introduce thermomechanical working as a strengthening scheme in any lead alloy intended for use at ambient temperature or above (the normal operating temperature for a lead acid storage battery can be as high as 160°F), one must consider warm-working effects, recovery, possible recrystallization, and creep. While to date no systematic investigation of the relationship between deformation and microstructure in lead alloys has been made, there are some pertinent observations from the literature pertaining to other alloy systems.

4.2.1. General processing approach

As we previously stated, high-temperature (up to 0.8 T_m) strength is greatly enhanced by the presence of a polygonized dislocation substructure which is additionally stabilized by an inert particle or stable precipitate dispersion. The interaction effect is best realized if the subgrain size is closely matched through processing, with the interparticle spacing of the dispersoid, and if the sub-boundary structure is made as well defined and perfect as possible. In terms of processing to establish such a substructure, the uniformity of strain during deformation is particularly important, especially with respect to resisting incipient recrystallization [51]. Processing which allows concentrated regions ("bands") of deformation cannot be used; localized deformation promotes accelerated recrystallization and grain growth during

subsequent heat-treatment or high temperature service [49, 51]. Many thermomechanical treatment schemes have utilized "sneaking-up" techniques to stepwise introduce dislocations by cold work in small amounts, often with intermediate anneals (so-called multiple mechanical-thermal treatments, or mmtt), to build up a high dislocation density while preventing recrystallization. Typically an alloy might be warm-worked at a temperature below that for rapid recrystallization, such that a polygonal substructure is formed based on the dispersoid or precipitate interparticle spacing [50]. The thermomechanical treatment may involve ageing followed by working, or the reverse, or some more complex scheme; the choice may depend on the relative temperature ranges for recrystallization and precipitation in a given system. In general, the warm working temperature must be high enough to ensure dispersed slip (homogeneously distributed deformation), but below the temperature at which recrystallization occurs [49]. Dispersed particles, if present during this deformation, may aid in the activation of multiple slip systems and, therefore, in the production of a more uniform dislocation density [51]. Dispersoids may also retard recrystallization, thereby extending the temperature range over which thermomechanical processing may be used to establish stable dislocation networks [71, 72].

4.2.2. Substructural strengthening of lead alloys

Thermomechanical processing schemes involving the principles cited above have not been applied to lead matrix materials with any exactness. Indeed, Greenough and Smith [73] and Gifkins [74, 75] have expressed doubt that lead alloys can be made to develop stable subgrain structures. However, a mmtt (multiple mechanical-thermal treatment) scheme for dispersion-strengthened metals, including lead, was patented in 1965 [76], and D–S lead products fabricated by working lead-matrix, dispersed-oxide material have been produced commercially [58, 60]. It seems likely that these processes, as well as many

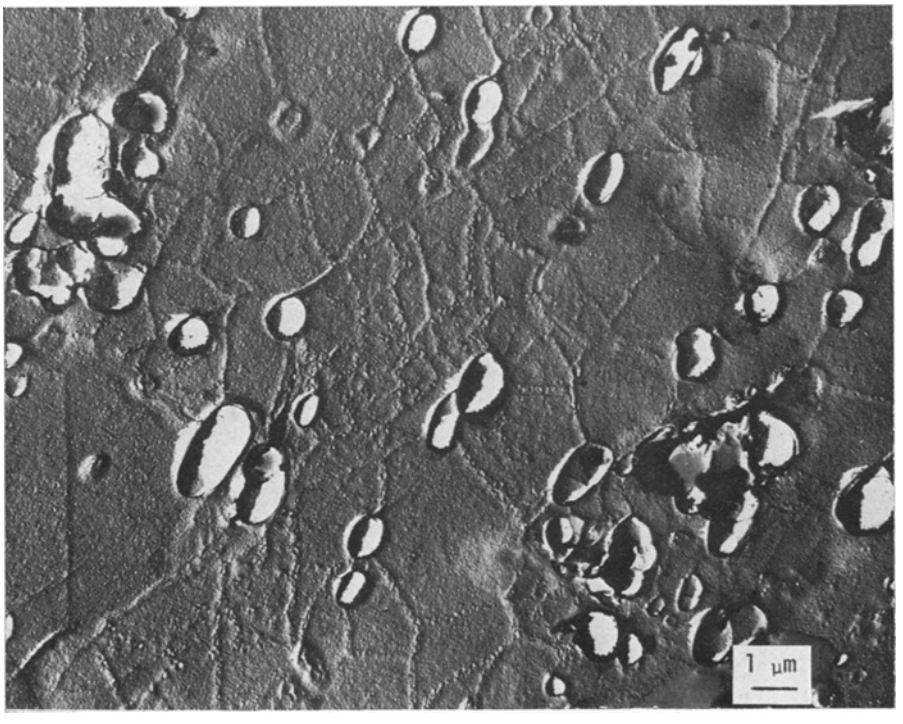

Figure 18 Substructure in Pb–1.4 wt % Cd–1.6 wt % Sb alloy thermomechanically processed by room temperature rolling and annealing at 200°F for 4 h. Fine particles of CdSb are precipitated along the polygonized subgrain boundaries. Replica transmission electron micrograph. × 7500. (Courtesy of M. M. Tilman, Bureau of Mines, Rolla Metallurgy Research Center.)

of the schemes cited earlier to produce dispersoids in lead matrices [59, 65, 68, 69, 77] do develop stable substructures similar to that described in the previous section, although no direct verifications have been presented. Recent replica electron microscopic studies by Tilman and Neumeier [78] have provided the first direct evidence that subgrain structures can be developed and stabilized in lead matrix materials. Deformed Pb–Cd–Sb alloys were shown to exhibit dramatic increases in creep resistance when cyclic deformation-annealing treatment (mmtt) was employed [78]; structural observations correlate this with development of polygonized subgrains associated with distributions of sub-micron-sized CdSb precipitate particles in this system (see Fig. 18).

5. Conclusions

It is apparent that there is great benefit to be obtained from development programs which are able to approach the problems cited using direct microstructural control. Electron microscopic observation techniques, which have proved to be powerful tools in numerous commercial alloy systems, have been used sparingly to study microstructural and submicrostructural features in lead alloys. Replica techniques have had some utilization, but the density of lead has inhibited the application of transmission electron microscopy (TEM) techniques. This may be an area in which high-voltage TEM may eventually play an important role.

Acknowledgements

The authors express their thanks to various individuals and organizations for contribution of helpful comments, research results, and data, including: M. M. Tilman, Rolla Metallurgy Research Center, Bureau of Mines; C. J. Hall, Chloride Technical Ltd; T. W. Caldwell, NL Industries; G. W. Mao and J. G. Larson, Gould, Inc; VARTA Batterie AG; and St. Joe Minerals Corporation. Particular appreciation is given to O. D. Sherby and C. M. Young, Stanford University, for helpful discussion. The work was supported in part by the Office of Naval Research (ONR) Naval Postgraduate School Foundation Research Program.

References

1. See for example: W. HOFMANN, "Lead and Lead Alloys" (English translation), (Springer-Verlag, New York and Berlin, 1970) pp. 341-57.
2. J. J. LANDER, *J. Electrochem. Soc.* **99** (1952) 339.
3. J. L. DAWSON, M. I. GILLIBRAND and J. WILKINSON, Preprint, Paper No. 1, 7th International Power Sources Symposium, Brighton, England (1970).
4. J. A. ORSINO and H. E. JENSON, Proceedings 21st Annual Power Sources Conference (1967) p. 60.
5. J. R. THOMAS and D. R. WOLTER, *ibid*, p. 64.
6. J. P. MALLOY, *ibid*, p.68.
7. E. E. SCHUMACHER and G. S. PHIPPS, *Trans. Electrochem. Soc.* **68** (1935) 309.
8. S. TUDOR, A. WEISSTUCH and S. H. DAVANG, *Electrochem. Technol.* **4** (1966) 406.
9. C. DROTSCHMANN, *Batteries (Holland)* **19** (1966) 851.
10. S. TUDOR, A. WEISSTUCH and S. H. DAVANG, *Electrochem. Technol.* **5** (1967) 21.
11. A. A. ABDUL AZIM and K. M. EL SOBKI, *Corrosion Sci.* **12** (1972) 371.
12. G. W. MAO, J. G. LARSON and P. RAO, *J. Electrochem. Soc.: Electrochem. Sci. and Tech.* **120** (1973) 11.
13. J. A. YOUNG and J. B. BARCLAY, Paper, 85th Convention Battery Council Internat. (1973).
14. W. SCHARFENBERGER and S. HENKEL, *Z. Metallk.* **64** (1973) 478.
15. E. HOEHNE and H. D. VON SCHWEINITZ, *Metallwortschaff* **21** (1942) 218.
16. H. W. KERR, *J. Inst. Metals* **99** (1971) 238.
17. J. D. WILLIAMS, *Metallurgia* **74** (1966) 105.
18. G. W. MAO and J. G. LARSON, *ibid* **76** (1968) 236.
19. "A Study of Lead Base Alloys", Armour Research Foundation Report No. ARF-2745-18, Oct. 9, 1962.
20. M. ABALLE and M. TORRALBA, *Rev. Met. (Spain)* **5** (1969) 385.
21. S. NISHIKAWA and T. TSUMURAYA, *Seisan Kenkyu (Japan)* **21** (1969) 596.
22. C. DROTSCHMANN, *Batteries (Holland)* **19** (1966) 876.
23. *Idem, ibid* **19** (1966) 899.
24. L. ARDUINI and L. BARONI, *Met. Ital.* **60** (1968) 437.
25. G. W. MAO, J. G. LARSON and P. RAO, *J. Inst. Metals* **97** (1969) 343.
26. R. NOZATO, *Bull. Univ. Osaka Prefect., Ser. A.* **16** (1967) 145.
27. E. PELZEL, *Metall.* **21** (1967) 23.
28. G. W. MAO, T. L. WILSON and J. G. LARSON, *J. Electrochem. Soc.: Electrochem. Tech.* **117** (1970) 1323.
29. T. L. WILSON and G. W. MAO, *Met. Trans.* **1** (1970) 2631.
30. A. KIROW, T. ROGATSCHEV and D. DENEW, *Metalloberflaeche* **26** (1972) 234.
31. L. N. LARIKOV and Y. F. YURCHENKO, *Ukr. Fiz. Zh.* **9** (1964) 1345.
32. P. RAO and G. W. MAO, *J. Inst. Metals* **100** (1972) 13.
33. G. W. MAO and P. RAO, *Br. Corros. J.* **6** (1971) 122.

34. V. I. BRYNTSEVA, Y. D. DUNAEV and G. Z. KIRYAKOV, *Izv. Akad. Nauk. Kaz. S.S.R. Ser. Khim* (1968) No. 3, 43-51.
35. V. I. BRYNTSEVA, Y. D. DUNAEV and G. Z. KIRYAKOV, *Zashchita Metal.* **5** (1969) 325.
36. J. VERNEY, *Metall.* **23** (1969) 836.
37. G. W. MAO, J. G. LARSON and P. RAO, *Metallography* **1** (1969) 399.
38. J. A. VONFRAUNHOFER, *Anticorrosion Methods Mater.* **15** (11) (1968), *ibid* **15** (12) (1968).
39. S. FELIU, L. GALAN and J. A. GONZALEZ, *Werkstoffe Korrosion* **23** (1972) 554.
40. A. M. HOWARD and E. WILLIHNGANZ, *Electrochem. Tech.* **6** (1968) 370.
41. R. LAGNEBORG, *Int. Met. Rev.* **17** (1972) 130.
42. O. D. SHERBY and P. M. BURKE, *Progr. Mat. Sci.* **13** (1967) 325.
43. R. JACKSON, H. J. CARVALHINOS and B. B. ARGENT, *J. Iron and Steel Inst.* **96** (1968) 210.
44. F. GAROFALO, "Fundamentals of Creep and Creep-Rupture in Metals" (Macmillan, New York, 1965) p. 33.
45. A. K. MUKHERJEE, J. E. BIRD and J. E. DORN, *Trans. ASM* **62** (1969) 155.
46. M. R. STAKER and D. L. HOLT, *Acta Met.* **20** (1972) 569.
47. C. M. YOUNG and O. D. SHERBY, *J. Iron and Steel Inst.* **101** (1973) 640.
48. O. D. SHERBY and C. M. YOUNG, private communication.
49. B. H. KEAR, J. M. OBLAK and W. A. OWCZARSKI, *J. Metals* **24** (6) (1972) 25.
50. J. M. OBLAK and W. H. OWCZARSKI, *Met. Trans.* **3** (1972) 617.
51. M. A. CLEGG and J. A. LUND, *ibid* **2** (1971) 2495.
52. P. R. STRUTT and R. S. POLVANI, *Scripta Met.* **7** (1973) 1221.
53. D. J. LLOYD and K. TANGRI, *Met. Sci. Eng.* **10** (1972) 75.
54. B. A. WILCOX and A. H. CLAUER, *Acta Met.* **20** (1972) 743.
55. F. L. VERSNYDER and M. E. SHANK, *Mat. Sci. Eng.* **6** (1970) 213.
56. J. D. EMBURY, B. A. WILCOX and A. H. CLAUER, *J. Inst. Metals* **100** (1972) 153.
57. D. H. ROBERTS, N. A. RATCLIFFE and J. E. HUGHES, *Powder Met.* **10** (1962) 132.
58. ST. JOSEPH LEAD COMPANY, bulletin, 1970.
59. ASSOCIATED ELECTRICAL INDUSTRIES, U.S. Patent 3 189 989, 20 May 1963.
60. ST. JOSEPH LEAD COMPANY, U.S. Patent 3 310 438, 17 February 1966.
61. J. A. LUND, D. TROMANS and B. N. WALKER, ILZRO Project LM-8 Final Report, January 1968.
62. F. V. LENEL, *Powder Met.* **10** (1962) 119.
63. H. C. WESSON, *Light Metals Metal Ind.* **28** (1965) 71.
64. M. M. TILMAN, R. L. CROSBY and D. H. DESY, *U.S. Bur. Mines Rep. Invest.* No. 7570 (1971).
65. ASSOCIATED ELECTRICAL INDUSTRIES, British Patent 1 122 823, 19 May 1966, *Met. Pat. J.* **8** (1968) No. 35.
66. H. LUCK, *Wiss. Z. Tech. Hochsch. Magdeburg* **14** (1970) 63.
67. J. WELLER and H. LUCK, *Wiss. Z. Tech. Univ. Dresden* **19** (1970) 629.
68. ELECTRIC AUTO-LITE CO., U.S. Patent 3 253 912, 20 May 1963, *Offic. Gaz. U.S. Pat. Office* **866** (1966) 1600.
69. J. LUCAS LTD., U.S. Patent 3 608 027, 29 July 1969, *Offic. Gaz. U.S. Pat. Office* **890** (1971) 1271.
70. ST. JOSEPH LEAD CO., U.S. Patent 3 416 918, 12 May 1966, *Offic. Gaz. U.S. Pat. Office Abstr. Section*, 17 December 1968, p. 884.
71. D. WEBSTER, D. D. CROOKS and A. E. VIDOZ, *Met. Trans.* **4** (1973) 2841.
72. D. WEBSTER, *Trans. ASM* **62** (1969) 936.
73. G. B. GREENOUGH and E. M. SMITH, *J. Inst. Met.* **77** (1950) 435.
74. R. C. GIFKINS, *J. Inst. Met.* **82** (1953-54) 39.
75. *Idem, ibid* **79** (1951) 233.
76. SHERRITT GORDON MINES LTD., U.S. Patent 3 366 515, 21 June 1965.
77. DOW CHEMICAL COMPANY, U.S. Patent 3 674 536, 6 February 1970, *Offic. Gaz. U.S. Pat. Office* **902** (1972) 1458.
78. M. M. TILMAN and L. A. NEUMEIER, *Met. Trans.* **4** (1973) 1997.

Received 12 February and accepted 3 May 1974.